

# Platelet Immobilization on Supported Phospholipid Bilayers for Single Platelet Studies

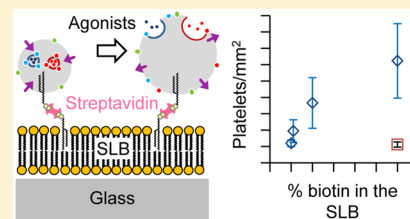
Eva Uhl,<sup>†</sup> Alessia Donati,<sup>†</sup> and Ilya Reviakine<sup>\*,†,‡</sup>

<sup>†</sup>Institute of Functional Interfaces (IFG), Karlsruhe Institute of Technology (KIT), Hermann-von-Helmholtz-Platz 1, 76344 Eggenstein-Leopoldshafen, Germany

<sup>‡</sup>Department of Bioengineering, University of Washington, Seattle, Washington 98105, United States

## S Supporting Information

**ABSTRACT:** The worldwide cardiovascular disease (CVD) epidemic is of grave concern. A major role in the etiology of CVDs is played by the platelets (thrombocytes). Platelets are anuclear cell fragments circulating in the blood. Their primary function is to catalyze clot formation, limiting traumatic blood loss in the case of injury. The same process leads to thrombosis in the case of CVDs, which are commonly managed with antiplatelet therapy. Platelets also have other, non-hemostatic functions in wound healing, inflammation, and tissue regeneration. They play a role in the early stages of atherosclerosis and the spread of cancer through metastases. Much remains to be learned about the regulation of these diverse platelet functions under physiological and pathological conditions. Breakthroughs in this regard are expected to come from single platelet studies and systems approaches. The immobilization of platelets at surfaces is advantageous for developing such approaches, but platelets are activated when they come in contact with foreign surfaces. In this work, we develop and validate a protocol for immobilizing platelets on supported lipid bilayers without activation due to immobilization. Our protocol can therefore be used for studying platelets with a wide variety of surface-sensitive techniques.



## INTRODUCTION

Platelets are small (2–4  $\mu\text{m}$ ) anuclear cell fragments circulating in the blood.<sup>1</sup> They maintain the integrity of the vascular bed,<sup>2,3</sup> catalyze clot formation to minimize traumatic blood loss when vascular integrity is compromised,<sup>1,4,5</sup> and orchestrate the inflammatory and wound-healing processes that follow the clotting stage.<sup>5–7</sup> Unfortunately, they also play a crucial role in cardiovascular disorders (CVDs), being involved in the development of atherosclerosis from the very early stages of the disease to the eventual thrombosis that causes heart attacks and stroke.<sup>8,9</sup> CVDs are currently the major cause of death worldwide, with more than 50% of patients dying as a result of consequences of atherosclerosis.<sup>10–12</sup> Antiplatelet therapy is widely used to manage CVDs,<sup>13</sup> but it incurs a bleeding risk.<sup>14–17</sup> The severity of the global CVD epidemic and the bleeding risks associated with the existing antiplatelet therapies continue to drive the search for therapeutic options with improved selectivity. Of particular interest are treatments that capitalize on platelets' regenerative functions. This, in turn, requires advances in understanding how platelet activity is regulated.

The history and state of the art of platelet research have been recently reviewed by Collier.<sup>18</sup> Much progress has been made in identifying agonists and antagonists and mapping out platelet-signaling pathways regulating platelet functions in the context of hemostasis and thrombosis. Questions of current interest include interactions between various signaling pathways<sup>19</sup> and the regulation of platelet secretion reactions. Understanding the organization of the signaling pathways is expected to aid in the

development of targeted antiplatelet therapies, while the secretion reactions are thought to be responsible for the regenerative and other nonhemostatic functions of platelets.<sup>7,20,21</sup> Breakthroughs in these directions are expected to come from single-platelet studies and systems approaches that would complement existing functional and flow cytometric assays.<sup>18</sup> Such approaches would benefit from the immobilization of platelets at surfaces and applications of sensitive surface analytical<sup>22</sup> and array technologies.<sup>23,24</sup> For example, we have recently reported the first single-platelet study with surface-immobilized platelets aimed at the analysis of platelet granule secretion.<sup>25</sup>

Immobilizing platelets at surfaces presents a problem: platelets are activated upon contact with artificial materials. An example of such activation is shown in Figure 1, where platelets adsorbed on glass are spread and express CD62P,<sup>26</sup> a marker signifying that a secretion reaction has taken place upon interaction with the surface of glass. Numerous examples of similar activation and spreading phenomena can be found in the literature.<sup>27–30</sup> The purpose of this study is to circumvent this well-known problem and devise a protocol for immobilizing purified platelets at surfaces while limiting their activation so that they can be used in further studies.

Our approach to immobilizing platelets is summarized in Figure 2. It relies on the surface-passivating properties of

Received: May 15, 2016

Revised: July 13, 2016

Published: July 20, 2016

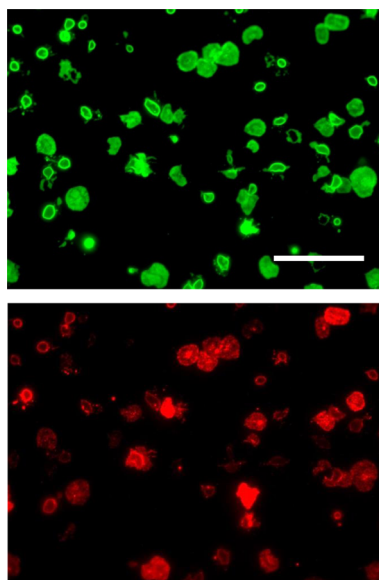


**Figure 1.** Platelets adhering to the bare glass surface are spread and activated. Purified platelets adhering to a bare glass surface were stained with the aCD41a antibody (green) and aCD62P antibody (red). Platelets are spread and express CD62P, which indicates activation. Scale bar: 40  $\mu\text{m}$ .

supported lipid bilayers (SLBs) on one hand and on the biotin–streptavidin interaction<sup>31</sup> for immobilization on the other hand. SLB formation, characterization, and properties, including those containing biotinylated lipids, have been described in detail in numerous publications by us and by others.<sup>32–37</sup> SLBs are known to passivate surfaces on short time scales (hours), preventing nonspecific protein adsorption<sup>38,39</sup> and cell adhesion.<sup>40</sup> This time scale is sufficient for the experiments with platelets, which take at most a few hours, because platelets are spontaneously activated during storage outside the body.<sup>41–43</sup> Some studies show that surface passivation with SLBs is superior to the standard serum albumin approach.<sup>44</sup> SLBs have formed the basis of a number of cell-based assays, in particular, in the area of immunology.<sup>45–47</sup> Thus, we prepared SLBs containing a biotinylated lipid on glass, introduced biotinylated lipids into the platelets, and linked the two together using streptavidin. Platelet biotinylation, the characterization of biotinylated platelets, and their interaction with streptavidin are described in detail in the **Results** section. Activation levels of the immobilized platelets and their response to agonists were then evaluated quantitatively using immunofluorescence microscopy against granule secretion marker CD62P and compared to flow cytometry results for platelets in solution.

## MATERIALS AND METHODS

**Materials.** *Monoclonal Antibodies and Protein-Conjugated Fluorochromes.* PerCP-Cy5.5-conjugated anti-CD41a, PE-conjugated anti-CD62P, V450-conjugated anti-CD63, FITC-conjugated PAC1, and BV605-conjugated phospholipid binding protein Annexin A5 (BD Biosciences, Heidelberg, Germany).

*Phospholipids.* DOPC (2-dioleoyl-*sn*-glycero-3-phosphocholine), NBD-PC (1-palmitoyl-2-[6-[(7-nitro-2-1,3-benzoxadiazol-4-yl)-amino]hexanoyl]-*sn*-glycero-3-phosphocholine), DPPE-cap-biotin 1,2-dipalmitoyl-*sn*-glycero-3-phosphoethanolamine-*N*-(cap biotinyl), and LRPE (1,2-dioleoyl-*sn*-glycero-3-phosphoethanolamine-*N*-(lissamine rhodamine B sulfonyl)) were purchased from Avanti Polar Lipids (Alabaster, AL).

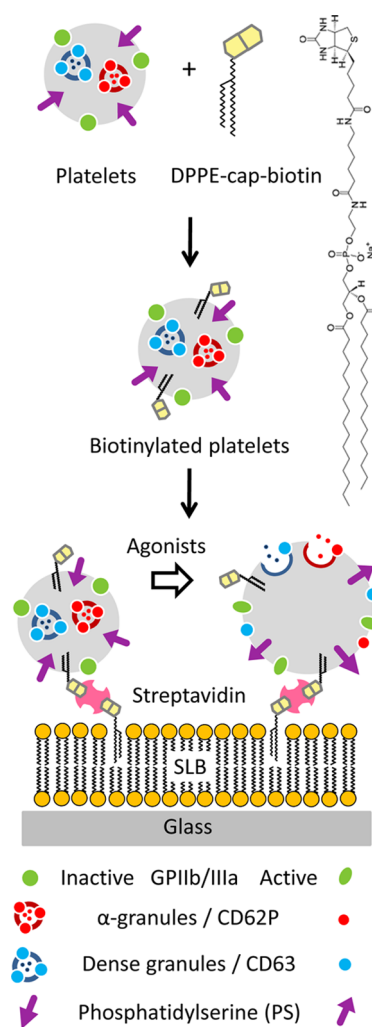


**Figure 2.** Study schematic. Platelets (gray spheres) purified from human blood were biotinylated by introducing DPPE-cap-biotin into their membranes. The structure of this lipid is shown in the figure and it is schematically represented with a yellow biotin headgroup and two black chains. Biotinylated platelets were immobilized on glass-supported lipid bilayers (SLBs) using the streptavidin–biotin link. Activation studies were conducted on the immobilized platelets by exposing them to agonists (TRAP in this study). Platelet activation entails changes in size as well as the secretion of granules and the consequent expression of granule-related activation markers CD62P (red filled circles) and CD63 (light-blue filled circles) on the platelet surface. It also entails the redistribution of phosphatidylserine (PS, purple arrowheads) and the activation of constitutively expressed integrin receptor GPIIb/IIIa (green circles and ellipses for the inactive and active forms, respectively). Small dots inside the granules represent granule contents secreted as a part of the activation process. In this study, CD62P expression was monitored to assess granule secretion in immobilized platelets by immunofluorescence microscopy. The response was compared to that of the platelets in solution analyzed by flow cytometry.

**Other Chemicals.** Acid citrate dextrose (ACD), calcium chloride hexahydrate  $\geq 99.0\%$ ,  $\alpha$ -D-glucose anhydrous 96%, magnesium chloride anhydrous  $\geq 98.0\%$ , potassium nitrate  $\geq 99\%$ , sodium chloride  $\geq 99.5\%$ , TRAP (thrombin receptor activating peptide), and PMA (phorbol 12-myristoyl acetate) were from Sigma-Aldrich (Steinheim, Germany). Water used for buffers and cleaning throughout this study was purified on a Arium Pro VF Ultrapure water system from Sartorius (Göttingen, Germany). HEPES (4-(2-hydroxyethyl)piperazin-1-ylethanesulfonic acid), 50% hydrogen peroxide, 28% ammonia solution, HCl, and

streptavidin were purchased from VWR International GmbH (Bruchsal, Germany). Fluorescein-conjugated streptavidin was purchased from Rockland (Limerick, PA, USA). Hellmanex III was from Hellma Analytics (Müllheim, Germany), BD cell fix solution was from BD Biosciences (Heidelberg, Germany), nitrogen gas 99.999% was from Air Liquide (Düsseldorf, Germany), and the addition-curing silicon glue Picodent Twinsil (speed 22) was from Picodent (Wipperfurth, Germany).

**Buffers.** Three buffers were used throughout the study. Buffer (A) contained 100 mM NaCl, 5 mM KCl, 5 mM glucose, 1 mM MgCl<sub>2</sub>, and 15 mM citrate, pH 6.5. Buffer (B) contained 145 mM NaCl, 5 mM glucose, 1 mM MgCl<sub>2</sub>, 10 mM HEPES, 5 mM KCl, and 2 mM CaCl<sub>2</sub>, pH 7.4. Buffer (C), used only for the SLB formation, contained 150 mM NaCl, 10 mM HEPES, and 2 mM CaCl<sub>2</sub>, pH 7.4. Buffers were prepared in nanopure water and autoclaved. Glucose was added to the autoclaved buffers, and the glucose-containing buffers were filtered through a 0.2- $\mu$ m-diameter syringe filter immediately before use.

**Methods. Preparation of Supported Lipid Bilayers (SLBs).** SLBs were prepared on freshly cleaned glass surfaces from unilamellar liposomes containing between 0 and 5% biotinylated lipid DPPE-cap-biotin and 0.5% chain-labeled NBD-PC. Liposomes were prepared in buffer C by extrusion through 50 nm pore diameter filters using the Avestin Lipofast hand-held extruder.<sup>48</sup> SLB preparation procedures have been described by our group in numerous previous publications.<sup>34,49,50</sup> Key factors for preparing good-quality SLBs are glass slide cleaning and the use of freshly prepared liposomes (less than 2 weeks old) that have been stored under argon or nitrogen.

Glass slides were cleaned with the modified RCA-1 cleaning procedure consisting of two steps: first, with H<sub>2</sub>O<sub>2</sub>/NH<sub>4</sub>OH/H<sub>2</sub>O (1:1:1.5) and then with H<sub>2</sub>O<sub>2</sub>/HCl/H<sub>2</sub>O (1:1:1.5) for 15 min at 50 °C. Slides were rinsed with nanopure water between and after the two cleaning steps. After the cleaning, the glass slides were stored under water until use in the SLB formation experiments. The storage time was never longer than overnight. Before the slides were removed, the air/water interface was cleaned of the adventitious contamination by pouring nanopure water into the tilted beaker while simultaneously pouring it out. This procedure was previously verified by XPS analysis of the surfaces and an examination of the quality of the resulting SLBs as a function of storage time (Camarero, S.; Reviakine, I. 2012, unpublished results). Clean glass slides were mounted in homemade Teflon cells using Picodent Twinsil two-component adhesive. Once the adhesive set (~2 min), the cells were filled with 400  $\mu$ L of buffer C, to which 10  $\mu$ L of a 5 mg/mL liposome suspension was added. SLBs were allowed to form for 1 h at room temperature, rinsed by exchanging the buffer (20 repetitions of 10 resuspensions of 100  $\mu$ L of fresh buffer (B) each), and warmed to 37 °C to prepare for platelet immobilization. Fluorescence recovery after photobleaching was performed on every SLB to examine its quality before the platelet experiments.

**Platelet Isolation and Purification from Human Whole Blood.** Blood collection was organized by the Medical Services, Karlsruhe Institute of Technology (Campus North, Eggenstein-Leopoldshafen, Germany). Study protocols were approved by the Ethics Commission of Baden-Württemberg (approval no. F-2014-077). Informed consent was obtained from all of the donors by the KIT medical staff. Donors were healthy volunteers without a history of exposure to antiplatelet medication (such as aspirin) or exposure to alcohol in the 2 weeks prior to collection. For each experiment, 10 mL of blood was drawn with a 21 gauge needle by venipuncture into two 5 mL glass BD Vacutainer tubes containing 0.5 mL of buffered 0.105 M trisodium citrate anticoagulant. The first 2 mL of blood was discarded during collection to avoid platelet activation by residual thrombin. The Vacutainer tubes were preheated to 37 °C prior to collection. Platelet purification was performed within 30 min of phlebotomy, during which time the blood-filled tubes were maintained at 37 °C. Platelets were purified by centrifugation. In the first step, platelet-rich plasma (PRP) was separated from the rest of the blood components by centrifugation at 40g for 25 min at 37 °C in a Sigma 3-30KHS centrifuge (Sigma Laborzentrifugen GmbH, Osterode am Harz,

Germany). Acid citrate dextrose (Sigma, Germany) was added to PRP in a ratio of 1:6 by volume, and it was incubated for 10 min at 37 °C. PRP was centrifuged for 20 min at 700g at 22 °C to pellet the platelets. They were resuspended in buffer (A) with gentle washing to remove as much of the plasma as possible, centrifuged for 10 min at 700g at 22 °C, and finally resuspended in buffer (B) at a concentration of  $\sim 1 \times 10^8$  platelets/mL. Platelet counts were determined with the ABX Pentra 60+ blood cell counter (Horiba Medical, Kyoto, Japan). These protocols have been previously established in our group.<sup>25,29,30,51</sup> Immediately after purification, the level of platelet activation and response to agonists was characterized by flow cytometry.

**Flow Cytometry.**<sup>52</sup> Flow cytometry was used to characterize the level of platelet activation and response to agonists immediately after purification as well as following biotinylation described in the next section. Platelets were identified by staining them with PerCP-Cy5.5-conjugated anti-CD41a antibodies. Activation markers were detected by staining the platelets with PE-conjugated anti-CD62P (P-selectin), V450-conjugated anti-CD63, FITC-conjugated PAC1 (antibody against the active conformation of GPIIb/IIIa), and BV605-conjugated Annexin A5 that binds phosphatidylserine. To prepare samples for flow cytometry analysis, 25  $\mu$ L of appropriately treated platelets (untreated, agonist-treated, biotinylated, etc.) in buffer B were incubated with the antibodies, appropriate isotype-matched controls, or annexin A5 for 30 min at 37 °C. Agonist treatment (0–150  $\mu$ M TRAP6, 10  $\mu$ M PMA) was performed for 30 min at 37 °C before the addition of the antibodies. Stained samples were diluted to 2 mL of buffer B and analyzed on the Attune acoustic focusing cytometer (Life Technologies, Darmstadt, Germany). Compensation parameters were set to avoid crossover fluorescence. Light-scattering and fluorescence data from 10 000 events were collected with the detectors set in logarithmic mode. Only CD41a positive events were considered in the analysis.

**Platelet Biotinylation.** Biotinylated lipid (DPPE-cap-biotin), alone or in a mixture with fluorescently labeled lipid Lissamine rhodamine B DOPE (LRPE), was incorporated into the platelets by an instantaneous dilution method. To this end, 0.5  $\mu$ L of lipid solution in ethanol was added to 100  $\mu$ L of a platelet suspension in buffer B and incubated for various periods of time (10–60 min, specified in the Results section). Lipid incorporation was evaluated by directly examining platelet fluorescence in experiments where LRPE was used or by adding fluorescently labeled streptavidin and analyzing platelets by flow cytometry in experiments where DPPE-cap-biotin was used alone. A lipid concentration of 0.065 mg/mL in ethanol solution (0.325  $\mu$ g/mL in the platelet suspension) was found to be appropriate for the immobilization experiments.

**Immobilization of Biotinylated Platelets.** Freshly prepared SLBs were incubated with 50  $\mu$ g/mL streptavidin in buffer C for 30 min. Excess streptavidin was removed by repeated rinsing with buffer B (22 repetitions of 10 resuspensions of 100  $\mu$ L). Samples were warmed to 37 °C. Biotinylated platelets were added to the SLBs and incubated for 1 to 3 h at 37 °C before staining with the fluorescent aCD41a and aCD62P antibodies. The staining was performed by adding 0.5  $\mu$ L of the aCD41a antibody solution diluted 1:3 in buffer B and 1  $\mu$ L of undiluted CD62P solution to a 400  $\mu$ L Teflon cell. Labeled samples were observed with fluorescence microscopy, and then excess platelets were removed by rinsing with buffer B (42 repetitions of 5 gentle resuspensions with 100  $\mu$ L of buffer). The number of remaining adhering platelets and their activation levels with and without agonist treatment were determined as described below.

**Fluorescence Microscopy and Image Analysis.** Fluorescence microscopy and FRAP were conducted using a Zeiss Axio Observer Z1 inverted fluorescence microscope (Zeiss, Jena, Germany) located in the laboratory of Dr. Cornelia Lee-Thedieck, equipped with a 63  $\times$  1.25 NA oil-immersion objective, a Colibri illumination system, a high-pressure Xe lamp, a set of filter cubes appropriate for the dyes used, an AxioCam MRm3 camera, and an environmental chamber (PeCon GmbH, Erbach, Germany). All experiments were performed at 37 °C. Images were recorded at the maximal resolution of 1388  $\times$  1040 pixels<sup>2</sup> corresponding to 142.10  $\times$  106.48  $\mu$ m<sup>2</sup>. Images were analyzed

using ImageJ version 1.42 software. Multichannel images were split. The aCD41a channel was used to identify platelets; images from this channel were converted to binary data by applying a threshold, and the particle analysis algorithm was used to determine the number of adhering platelets and to define a mask that was then used to determine the average fluorescence intensities of the platelets in the aCD62P channel. This reflected their activation levels.

## RESULTS

**Platelet Isolation, Purification, and Biotinylation.** The starting point for our experiments was citrate anticoagulated whole human blood. Platelets were purified by a series of centrifugation and washing steps described in Figure S1 in the Supporting Information, yielding a suspension of purified platelets in buffer B with a platelet concentration of  $10^8$  mL<sup>-1</sup>. Red blood cell concentrations in the purified platelet samples were below the levels of detection of the equipment, and white blood cell contamination did not exceed  $10^5$  mL<sup>-1</sup>. Freshly purified platelets were analyzed by flow cytometry to determine their activation levels and response to agonists such as TRAP and PMA. An example of such a measurement is presented in Figure 3A, where it is shown how the fractions of activated platelets were calculated from the fluorescence-intensity histograms. These are plotted in Figure 3B for the unstimulated and agonist-stimulated platelets, together with platelets that undergo biotinylation as described below. (The corresponding scatter plots are shown in Figure S2 in the Supporting Information.)

Freshly purified and characterized platelets were then used in biotinylation and immobilization experiments. To introduce biotin into the platelets, we chose to incorporate a biotinylated lipid into their membrane by the instant dilution method. (Others have previously used a chemical approach.<sup>53</sup>) This was achieved by adding 0.5  $\mu$ L of the biotinylated lipid, DPPE-cap-biotin, solution in ethanol to 100  $\mu$ L of the freshly purified platelet solution. The final ethanol concentration in the platelet solution was thus 0.5%. The first step was to choose the appropriate lipid concentration. To this end, fluorescently labeled LRPE was used as a reporter molecule, and solutions of 0.013, 0.065, 0.13, and 1.3 mg/mL of the 1:1 LRPE/DPPE-cap-biotin mixture in ethanol were mixed with the platelet solutions to yield final lipid concentrations of 0.065, 0.325, 0.65, and 6.5  $\mu$ g/mL, respectively. Labeled platelets were allowed to adsorb on glass and stained with aCD41a antibody for identification. The criteria that were used to select the appropriate lipid concentrations were the homogeneity of the aCD41a staining and the visibility of LRPE. In some experiments, mixtures of LRPE and DPPE-cap-biotin were used, and platelets were also labeled with fluorescently labeled streptavidin to examine the visibility of the label. The results are shown in Figure S3 in the Supporting Information. On the basis of these experiments, a DPPE-cap-biotin concentration of 0.325  $\mu$ g/mL was chosen, achieved by adding 0.5  $\mu$ L of 0.065 mg/mL DPPE-cap-biotin solution in ethanol to 100  $\mu$ L of platelets. For the  $10^8$  platelets/mL, this leads to  $\sim 2 \times 10^6$  lipid molecules per platelet at the most. A conservative estimate of the fraction of the added lipids relative to the total number of lipids in the platelet membrane can be made. Assuming spherical geometry, a platelet diameter of  $\sim 4$   $\mu$ m, and the area per molecule of a lipid of  $\sim 72$   $\text{\AA}^2$ , the fraction of the lipid incorporated is  $\sim 1\%$ . This is an upper limit, since the area of the platelet membrane is significantly larger than that of a sphere of equivalent diameter due to the extensive membrane area stored in the open canalicular system.

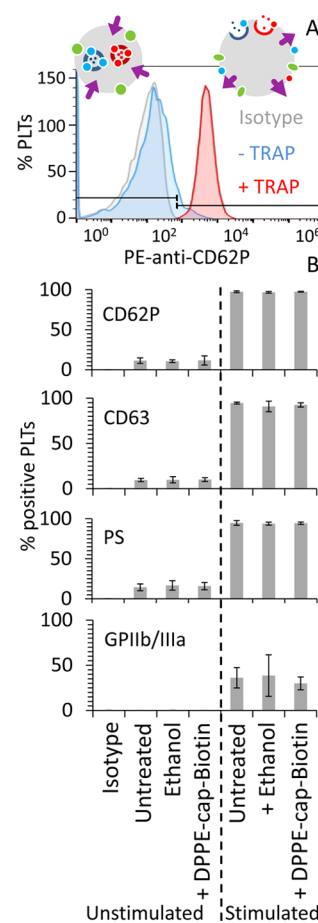


**Figure 3.** Characterization of the purified platelets by flow cytometry. (A) An example of a histogram showing the fraction of platelets with a given fluorescence intensity of the aCD62P-PE antibody under different conditions: gray, isotype; blue, unstimulated platelets; and red, agonist (TRAP)-stimulated platelets. The peak in fluorescence intensity shifts to the right upon TRAP treatment, indicating antibody binding to the CD62P expressed on the surfaces of the activated platelets. Black brackets indicate gates used to calculate activated platelet fractions. Schematic diagrams of platelet activation are shown above the histograms. The color scheme is the same as in Figure 2. (B) Fractions of platelets expressing CD62P, CD63, PS, and activated GPIIb/IIIa were calculated from the flow cytometry data as described in (A) in untreated platelets, platelets treated with ethanol alone (vehicle), or the solution of DPPE-cap-biotin in ethanol, that was either unstimulated or stimulated with an agonist. TRAP was used as an agonist for CD62P, CD63, and PS; PMA was used for GPIIb/IIIa. PS expression was determined using annexin A5 binding. Relevant antibodies were used for other markers. Error bars are standard deviations from 11 experiments with 6 different donors.

The next step was to examine the effect of lipid addition on platelet activation. To this end, the expression of the four activation markers on freshly purified platelets treated with ethanol with or without dissolved DPPE-cap-biotin was analyzed by flow cytometry. The results are shown in Figure 3B. No effect of ethanol or of the lipid on the marker expression levels could be observed. The ability of the platelets to respond to agonists (TRAP or PMA) was similarly unaffected by the addition of ethanol alone or of the solution of DPPE-cap-biotin in ethanol.

The last step in the biotinylation process was to analyze biotin exposure on the biotinylated platelets using fluorescently labeled streptavidin and the effect of streptavidin binding on the

activation of platelets. This was done using flow cytometry with fluorescently labeled streptavidin as a reporter, as well as antibodies against CD62P and annexin A5 to detect phosphatidylserine (PS). The results are shown in Figure 4. The corresponding scatter plots are shown in Figure S2 in the Supporting Information.

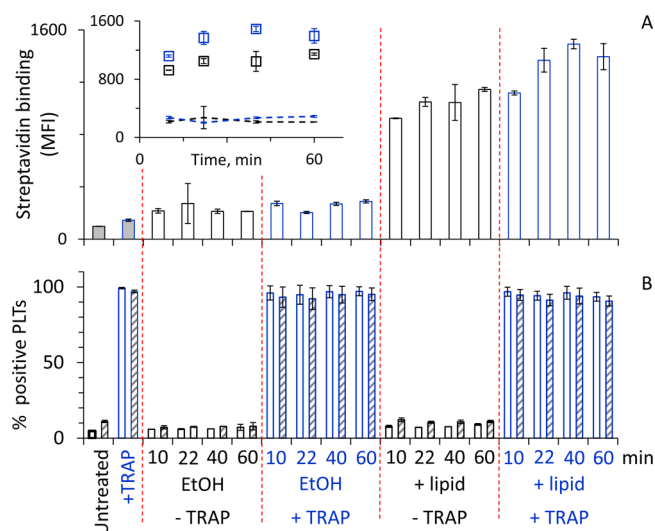


**Figure 4.** Analysis of biotinylated platelets by flow cytometry. (A) Median fluorescence intensities of platelets interacting with fluorescently labeled streptavidin. (B) Fraction of platelets expressing CD62P (open bars) or PS (diagonally hatched bars). In both panels, the blue bars (open squares in the inset) refer to agonist-stimulated platelets, while the black bars (open squares) refer to platelets that were not stimulated with the agonist (TRAP). Unstimulated platelets were incubated with ethanol (vehicle) or the solution of DPPE-cap-biotin in ethanol for 10, 22, 40, or 60 min, followed by incubation with fluorescent streptavidin and fluorescently labeled antibody against CD62P or annexin A5 to reveal PS expression. Some of the platelets were stimulated with TRAP before the incubation with the antibodies. Different measurement groups are separated with dashed red lines for clarity. Also included in the plots are the results for unstimulated and agonist-stimulated platelets that were not exposed to either ethanol or lipid but were otherwise treated in an identical manner for 60 min and then exposed to streptavidin; they appear in the leftmost group. The inset in (A) depicts the time dependence of the biotinylation revealed by streptavidin binding to the platelets incubated with the solution of the DPPE-cap-biotin lipid in ethanol for different time periods. Dashed lines refer to the ethanol alone controls. Error bars are standard deviations.

In Figure 4A, we present median fluorescence intensities (MFIs) of the platelets labeled with fluorescent streptavidin. The MFI values are significantly higher in the case of platelets treated with DPPE-cap-biotin than in the case of platelets that were exposed only to the vehicle (ethanol) or not exposed to either of the two reagents (controls). This is also visible in the inset, which reveals an increase in the MFI as a function of the time platelets were incubated with the biotinylated lipid solution. No such increase can be seen in the case of platelets incubated with ethanol alone for different amounts of time. These results are indicative of the specific binding of streptavidin to biotinylated platelets. More streptavidin appears to bind to TRAP-treated platelets than to otherwise identically handled platelets not treated with TRAP.

In the case of labeling platelets with fluorescent streptavidin, we chose to present the MFI values instead of calculating

labeled platelet fractions, as we do when we report the extent of platelet activation. This is because the case of streptavidin labeling is somewhat different from that of antibody binding to an activation marker. Activated platelet fractions are calculated on the basis of a threshold value of fluorescence intensity set using the isotype control (Figure 3A). Because there is no isotype control, the threshold value is not well-defined. The 100% binding is not defined either because it depends on the amount of DPPE-cap-biotin incorporated into the platelet membranes.

Fractions of platelets expressing activation markers CD62P and PS as a result of their exposure to DPPE-cap-biotin for different amounts of time and then to streptavidin are examined in Figure 4B. No effect of these treatments on the expression of either marker is observed. These treatments also do not interfere with the response of platelets to TRAP.

**Platelet Immobilization on Biotinylated SLBs.** Biotinylated SLBs were prepared from unilamellar liposomes on freshly cleaned glass surfaces (Materials and Methods) according to standard protocols previously used in our laboratory.<sup>34,35,49,50,54</sup> Prior to platelet immobilization, the SLB quality was verified qualitatively by fluorescence recovery after photobleaching, the results of which are shown in Figure S4 in the Supporting Information.

To immobilize platelets on the SLBs, we chose to first incubate the SLBs with streptavidin and then to add biotinylated platelets. This was done to avoid the need for separating excess streptavidin from the platelets by centrifugation, which could lead to additional platelet activation. Excess streptavidin was removed from the SLBs by simple rinsing prior to incubation with the platelets. The results are shown in Figure 5. Most of the platelets visible in the samples are removed after rinsing; only a few attached platelets remain (Figure 5A). The number of attached platelets increases with the biotin content of the SLBs (Figure 5B), further supporting that the binding is specific.

The nonspecific adhesion of platelets was examined by analyzing the number of platelets remaining on the SLBs after rinsing for the SLBs without DPPE-cap-biotin (pure DOPC) or for SLBs containing DPPE-cap-biotin but without the added streptavidin (Figure 5B). That number was relatively small,  $\sim 100\text{--}200$  PLTs/ $\text{mm}^2$ , compared to  $\sim 2.6 \times 10^3$  PLTs/ $\text{mm}^2$  on SLBs containing 1% DPPE-cap-biotin. This nonspecific adhesion is probably due to the defects in the bilayers.

No motion of immobilized platelets during experiments was detected.

**Analysis of Immobilized Platelet Activation.** To investigate the level of activation of the immobilized platelets and their response to platelet agonist analogue TRAP, immobilized platelets were treated with various TRAP concentrations (between 0 and 150  $\mu\text{M}$ ) and stained with aCD62P. Representative images are shown in Figure 6A. The number of platelets staining positive for CD62P increases with the TRAP concentration. The platelet shape and size also change.

Figure 6B shows histograms of fluorescence intensities due to the aCD62P staining for platelets treated with three different TRAP concentrations. A shift of the histograms to the right (higher intensities) is visible as a function of TRAP concentration. This situation is similar to that found in flow cytometry with platelets in solution (Figure 3A). The histograms shown in Figure 6B were used to define a threshold for calculating the fraction of activated platelets (dashed line):

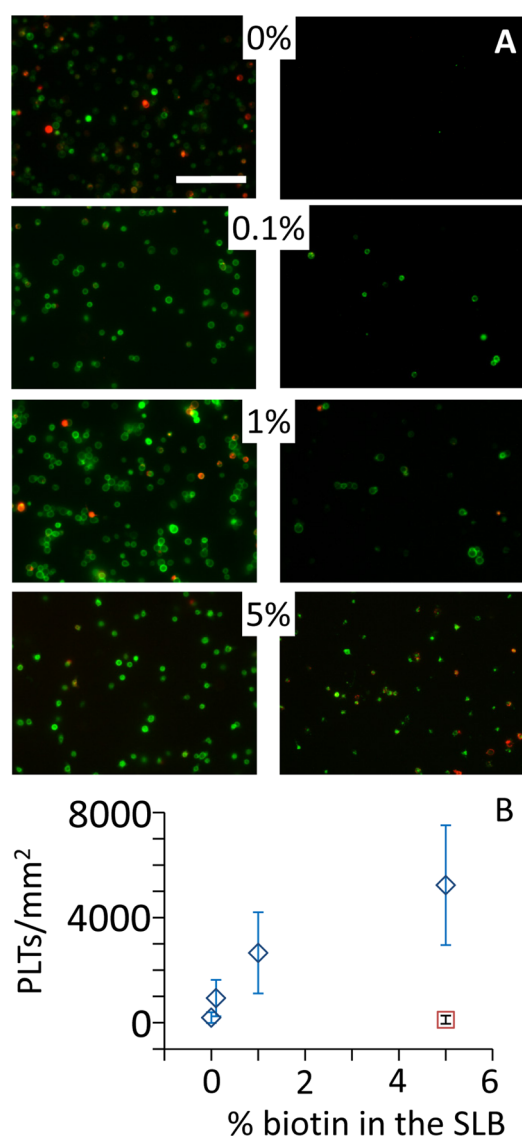


**Figure 5.** Immobilization of biotinylated platelets on the biotinylated SLBs. (A) Immunofluorescence microscopy images of platelets incubated with SLBs containing various amounts of DPPE-cap-biotin. The fraction of this lipid in the SLBs is indicated on the figure. Platelets were stained with the aCD41a (green) and aCD62P (red) antibodies for identification and to reveal the level of activation, respectively. Left: before rinsing. Right: after rinsing. The scale bar in the top-left image is 40  $\mu\text{m}$ . (B) The number of platelets remaining on the surface after rinsing is plotted as a function of the DPPE-cap-biotin content in the SLBs (blue rhombi). Error bars are standard deviations obtained from five to nine individual experiments with each SLB composition with blood from five different donors. Red square: a series of control experiments where no streptavidin was added to the SLB prior to the addition of the platelets. Error bars are standard deviations from three individual SLBs with blood from one donor.

platelets with fluorescence intensity above the threshold are considered to be activated, while platelets with fluorescence intensity below the threshold are considered to be resting. This is a similar procedure to that used in the analysis of flow cytometry data, where the threshold is defined on the basis of the locations of the fluorescence intensity peaks of the isotype-matched control and of the activated platelets (Figure 3A).

Fractions of activated platelets obtained with the above procedure from the immunofluorescence microscopy images

and flow cytometry are plotted together as a function of TRAP concentration in Figure 6C. Qualitatively similar responses are observed in both cases. To make the comparison more quantitative, the results of the two methods are plotted against each other in Figure 6D. The relationship between the two sets of results is linear, with a slope of  $0.85 \pm 0.03$  and an  $R^2$  value of 0.91. This indicates that immobilized platelets and platelets in solution behave in a similar manner with respect to CD62P expression when challenged with TRAP. Identical behavior is expected to give rise to a slope of 1.

A similar analysis was performed in the case of unstimulated platelets, with a similar result (Figure S5 in the Supporting Information).

## DISCUSSION

The aim of this study was to immobilize platelets on the surface of glass without activation that adhesion to the surface normally induces (Figure 1). This was achieved by relying on the well-known ability of SLBs to passivate surfaces of inorganic materials.<sup>32,38–40</sup> Here, it is important to remember that experiments with purified platelets can be done only on the scale of a few hours at the most because of their spontaneous activation. Therefore, the passivating capacity of the SLB is sufficient. Linkage to the SLB was provided by the biotin/streptavidin interaction, with a biotinylated lipid incorporated into the SLB at the formation stage and into the platelets by the instant dilution method (Figure 2).

Throughout the labeling and immobilization procedure (Figure 2), it was important to verify that platelet activation remained minimal at every step. Particularly important in the context of our future goal of investigating platelet secretion was the  $\alpha$ -granule specific surface marker, CD62P (P-selectin).<sup>26</sup> Indeed, we showed that the expression level of this marker was not elevated above the level already present on the freshly purified platelets as a result of the introduction of the biotinylated lipid (Figure 3) or because of the addition of streptavidin to the biotinylated platelets (Figure 4B). PS expression was similarly unaffected (Figure 4B).

The streptavidin-mediated immobilization of biotinylated platelets on biotin-containing SLBs was shown to be specific because the number of immobilized platelets (i) depended on the amount of biotin in the SLBs and (ii) was significantly higher than the number of platelets adhering on the biotin-free or streptavidin-free SLBs (Figure 5).

Finally, the activation and activation behavior of the immobilized platelets was similar to that of the platelets in solution. This was the case for the freshly purified, unstimulated platelets (Figure S5 in the Supporting Information) as well as for the platelets treated with different concentrations of TRAP (Figure 6). Here, as throughout the article, platelet activation is defined in terms of the number of platelets expressing CD62P at a level above the threshold defined for fluorescence microscopy and flow cytometry as described in Figures 6D and 3A, respectively.

Some differences between the activation of the immobilized platelets and platelets in solution were noted. It appears that immunofluorescence microscopy is less sensitive to platelet activation than flow cytometry. This is apparent from the trends visible in Figure 6D and in Figure S5 in the Supporting Information, where the two methods are compared directly. The origin of the difference is not entirely clear, but these differences are small.

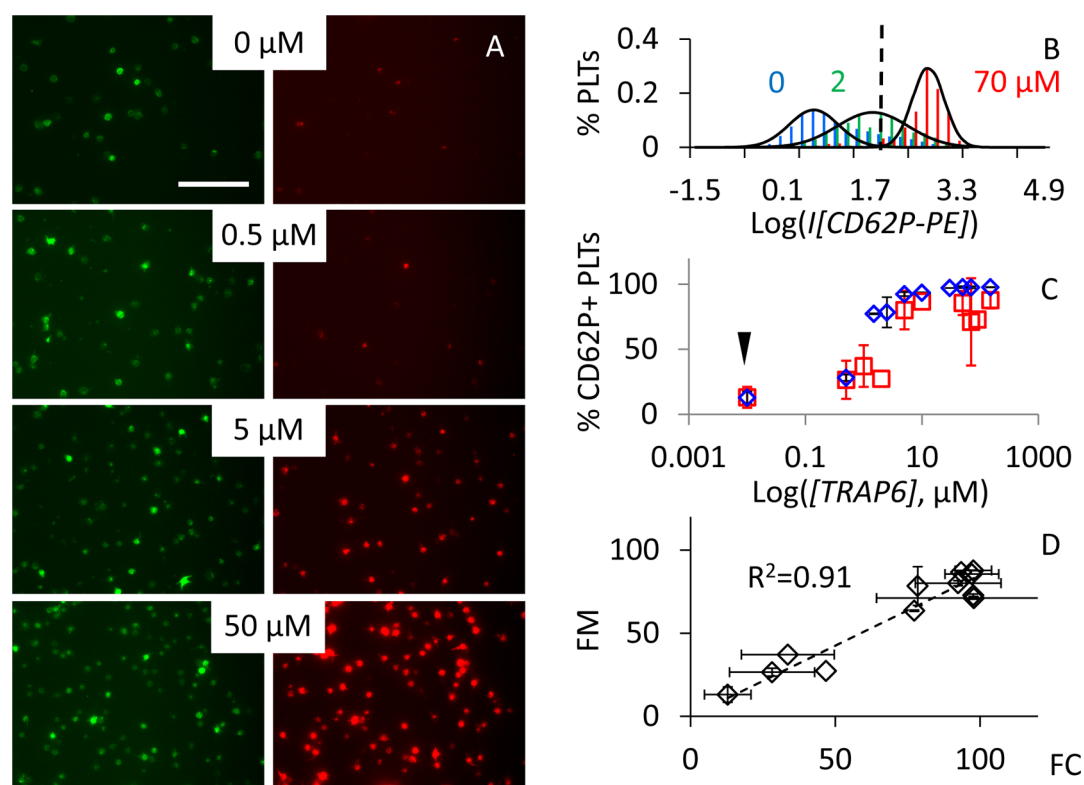


**Figure 6.** Analysis of immobilized platelet activation. (A) Immunofluorescence microscopy images of platelets immobilized on SLBs containing 1% DPPE-cap-biotin. Platelets were stained with aCD41a (green) for identification and aCD62P (red) to evaluate their activation levels. Numbers indicate TRAP concentrations used to stimulate platelets. Representative images from different experiments are shown. (B) Fluorescence intensity histograms obtained from images such as those shown in (A). Blue, 0  $\mu\text{M}$  TRAP (10 experiments); green, 1  $\mu\text{M}$  (2 experiments); red, 70  $\mu\text{M}$  (3 experiments). The histograms shift to the right with increasing TRAP concentration, reflecting an increasing platelet activation level. The dashed line indicates the threshold (1.9) that was used to calculate the fractions of platelets expressing CD62P in the subsequent analysis of the fluorescent images. (C) The percentage of platelets expressing CD62P calculated from the flow cytometry measurements for platelets in solution (blue) and immunofluorescence microscopy for the immobilized platelets (red) plotted as a function of TRAP concentration. Error bars are standard deviations. Arrowhead: unstimulated platelets (0  $\mu\text{M}$  TRAP). The raw flow cytometry data is shown in Figure S6 in the [Supporting Information](#). (D) Same as (C), with the fluorescence microscopy (FM) data plotted vs the flow cytometry data (FC). The dashed line is a linear fit to the data with a slope of  $0.85 \pm 0.03$ .

It is well known that phospholipids in membranes of cell are distributed asymmetrically, with aminophospholipids such as PS and PE favoring the inner membrane leaflet.<sup>55</sup> The asymmetric distribution is maintained through the action of ATP-dependent flippases.<sup>56</sup> This subject had been comprehensively reviewed by Daleke.<sup>57</sup> Therefore, a particular concern with using a PE-based phospholipid to introduce the biotin into the platelets is its possible internalization. Such a process would manifest itself as a decrease in the amount of available biotin with time. On the contrary, the results presented in [Figure 5A](#) (inset) show that the amount of exposed biotin increases with the time platelets are incubated with the solution of DPPE-cap-biotin in ethanol over a time period of 1 h. There is no evidence of a decrease in the amount of biotin exposed on the platelet surface during this time. There are two likely reasons for this. First, flippases are rather selective with respect to the lipid headgroup, favoring PS over PE for transmembrane transport, whereas the rate of transport of phosphatidylcholine (PC) is very small.<sup>58</sup> In an experiment where spin-labeled phospholipids were added to the red blood cells, PS was transported to the inner leaflet within an hour and PE, within 8 h, and the transport of PC continued over a period of 18 h.<sup>58</sup> Morrot et al. furthermore showed that the progressive methylation of the primary amine from PE to PC reduced the rate of lipid

transport.<sup>58</sup> It can be seen in [Figure 2](#) that the amine group of PE is used to attach the biotin and the spacer. Second, the biotinylated headgroup with the spacer is rather bulky, further limiting the ability of the protein to transport this lipid.

The SLB-based approach we use to immobilize platelets on a surface is very flexible and versatile. It can be combined with patterning to create arrays<sup>47,59–63</sup> or with microfluidic approaches to be used under flow.<sup>64,65</sup> In particular, their intrinsic mobility can be combined with flow to simulate transport.<sup>64</sup> Biologically active substances relevant to platelet physiology, such as platelet activating factor or phosphatidylserine, can also be readily incorporated into the SLBs.

Potentially, other surface-passivation methods could be used, in particular, the ones based on PEGylation of the surface. It may be worth comparing the efficiency and the flexibility of the different methods in view of the knowledge that blood in contact with PEGylated surfaces continues to clot<sup>66</sup> and that plasma proteins adsorb to them.<sup>67</sup> Whether these phenomena are interrelated is not clear; however, zwitterionic lipids (such as the ones we use in the SLBs) also make up the outer leaflets of cell membranes.<sup>68,69</sup> One may speculate that for this reason they are more suitable than PEG when favorable interactions with volatile biological entities are sought.

## CONCLUSIONS

We developed a method to immobilize purified platelets at surfaces with limited activation in addition to that incurred by the purification itself. Platelets immobilized in this manner can be used in further studies. Our approach offers numerous new possibilities for further experimentation with platelets using surface analytical techniques.

## ASSOCIATED CONTENT

### Supporting Information

The Supporting Information is available free of charge on the ACS Publications website at DOI: 10.1021/acs.langmuir.6b01852.

Platelet isolation from whole blood, flow cytometry scatter plots, estimation of the DPPE-cap-biotin concentration needed for platelet biotinylation, supported lipid bilayer characterization, correlative analysis of surface-immobilized and solution-phase unstimulated platelets, and CD62P expression as a function of TRAP concentration in purified platelets measured by flow cytometry (PDF)

## AUTHOR INFORMATION

### Corresponding Author

\*E-mail: Ilya.Reviakine@kit.edu.

### Author Contributions

I.R. and A.D. designed the study, E.U. performed the experiments, E.U. and A.D. analyzed the data, I.R. and E.U. wrote the manuscript, and I.R. supervised the work.

### Notes

The authors declare no competing financial interest.

## ACKNOWLEDGMENTS

We thank the Biointerfaces in Technology and Medicine (BIF-TM) program of the Helmholtz Association (Germany) for financial support, Dr. Med. Volker List and Ms. Ingrid Schaefer (KIT, Germany) for organizing blood collection and testing, Mr. Michael Horisberger (Paul Scherrer Institut, Villigen, Switzerland) for the TiO<sub>2</sub>-coated glass coverslips, Prof. Matthias Franzerb (KIT) and Dr. Cornelia Lee-Thedieck (KIT) for support and access to the relevant equipment.

## REFERENCES

- (1) Michelson, A. D. *Platelets*, 3rd ed.; Academic Press: London, 2013.
- (2) Hess, H.; Marshall, M. Influence of platelets on the integrity of the vessel wall. *Adv. Exp. Med. Biol.* **1975**, *63*, 393–8.
- (3) Ho-Tin-Noe, B.; Demers, M.; Wagner, D. D. How platelets safeguard vascular integrity. *J. Thromb. Haemostasis* **2011**, *9*, 56–65.
- (4) Monroe, D. M.; Hoffman, M.; Roberts, H. R. Platelets and thrombin generation. *Arterioscler., Thromb., Vasc. Biol.* **2002**, *22* (9), 1381.
- (5) Vieira-de-Abreu, A.; Campbell, R. A.; Weyrich, A. S.; Zimmerman, G. A. Platelets: versatile effector cells in hemostasis, inflammation, and the immune continuum. *Semin. Immunopathol.* **2012**, *34* (1), 5–30.
- (6) Eppley, B. L.; Pietrzak, W. S.; Blanton, M. Platelet-Rich Plasma: A Review of Biology and Applications in Plastic Surgery. *Plast. Reconstr. Surg.* **2006**, *118* (6), 147E–159E.
- (7) Nurden, A. T. Platelets, inflammation and tissue regeneration. *Thromb. Haemostasis* **2011**, *105*, S13.
- (8) Ruggeri, Z. M. Platelets in atherothrombosis. *Nat. Med.* **2002**, *8* (11), 1227–34.

(9) Kaplan, Z. S.; Jackson, S. P. The role of platelets in atherothrombosis. *Hematology Am. Soc. Hematol Educ Program* **2011**, *2011*, 51–61.

(10) WHO Cardiovascular Diseases Fact Sheet 317 <http://www.who.int/mediacentre/factsheets/fs317/en/>.

(11) *Global Atlas on Cardiovascular Disease Prevention and Control*: World Health Organization: Geneva, 2011; p 164.

(12) Tardif, J.-C. Coronary artery disease in 2010. *Eur. Heart J. Suppl.* **2010**, *12*, C2–C10.

(13) Jackson, S. P.; Schoenwaelder, S. M. Antiplatelet therapy: in search of the 'magic bullet'. *Nat. Rev. Drug Discovery* **2003**, *2* (10), 775–89.

(14) Patni, R.; Nawaz, M. A.; Macys, A.; Chan, K. M.; Punjabi, P. Assessment of platelet function in patients on antiplatelet therapy undergoing cardiac surgery: a review. *Heart, Lung Circ.* **2012**, *21* (8), 455–62.

(15) Holmes, D. R., Jr.; Kereiakes, D. J.; Kleiman, N. S.; Moliterno, D. J.; Patti, G.; Grines, C. L. Combining antiplatelet and anticoagulant therapies. *J. Am. Coll. Cardiol.* **2009**, *54* (2), 95–109.

(16) Schomig, A.; Sarafoff, N.; Seyfarth, M. Triple antithrombotic management after stent implantation: when and how? *Heart* **2009**, *95* (15), 1280–5.

(17) Paikin, J. S.; Wright, D. S.; Eikelboom, J. W. Effectiveness and safety of combined antiplatelet and anticoagulant therapy: A critical review of the evidence from randomized controlled trials. *Blood Rev.* **2011**, *25* (3), 123–129.

(18) Collier, B. S. Historical perspective and future directions in platelet research. *J. Thromb. Haemostasis* **2011**, *9*, 374–95.

(19) Reviakine, I. New horizons in platelet research: Understanding and harnessing platelet functional diversity. *Clin. Hemorheol. Microcirc.* **2015**, *60* (1), 133–152.

(20) Leslie, M. Beyond Clotting: The Powers of Platelets. *Science* **2010**, *328* (5978), 562–564.

(21) Whiteheart, S. W. Platelet granules: surprise packages. *Blood* **2011**, *118* (5), 1190–1.

(22) Hook, F.; Kasemo, B.; Grunze, M.; Zauscher, S. Quantitative Biological Surface Science: Challenges and Recent Advances. *ACS Nano* **2008**, *2* (12), 2428–2436.

(23) Di Carlo, D.; Lee, L. P. Dynamic single-cell analysis for quantitative biology. *Anal. Chem.* **2006**, *78* (23), 7918–7925.

(24) Yarmush, M. L.; King, K. R. Living-Cell Microarrays. *Annual Review of Biomedical Engineering*; Annual Reviews: Palo Alto, CA, 2009; Vol. 11, pp 235–257.

(25) Donati, A.; Kustanovich, K.; Jeffries, G.; Jesorka, A.; Reviakine, I. Studying Platelet Activation at the Single Platelet Level. *Anal. Chem.* **2016**, Submitted for publication.

(26) Stenberg, P. E.; McEver, R. P.; Shuman, M. A.; Jacques, Y. V.; Bainton, D. F. A platelet alpha-granule membrane protein (GMP-140) is expressed on the plasma membrane after activation. *J. Cell Biol.* **1985**, *101* (3), 880.

(27) Fritz, M.; Radmacher, M.; Gaub, H. E. In vitro activation of human platelets triggered and probed by atomic force microscopy. *Exp. Cell Res.* **1993**, *205* (1), 187–90.

(28) Braune, S.; Alagoz, G.; Seifert, B.; Lendlein, A.; Jung, F. Automated image-based analysis of adherent thrombocytes on polymer surfaces. *Clin. Hemorheol. Microcirc.* **2012**, *52* (2–4), 349–55.

(29) Gupta, S.; Reviakine, I. Platelet activation profiles on TiO<sub>2</sub>: effect of Ca<sup>2+</sup> binding to the surface. *Biointerphases* **2012**, *7*, 28.

(30) Gupta, S.; Donati, A.; Reviakine, I. Differences in intracellular calcium dynamics cause differences in  $\alpha$ -granule secretion and phosphatidylserine expression in platelets adhering on glass and TiO<sub>2</sub>. *Biointerphases* **2016**, *11*, 029807.

(31) Wilchek, M.; Bayer, E. A. Avidin-biotin technology ten years on: has it lived up to its expectations? *Trends Biochem. Sci.* **1989**, *14*, 408–412.

(32) Sackmann, E. Supported membranes: Scientific and practical applications. *Science* **1996**, *271* (5245), 43–48.

- (33) Richter, R. P.; Berat, R.; Brisson, A. R. Formation of solid-supported lipid bilayers: An integrated view. *Langmuir* **2006**, *22* (8), 3497–3505.
- (34) Reviakine, I.; Brisson, A. Formation of supported phospholipid bilayers from unilamellar vesicles investigated by atomic force microscopy. *Langmuir* **2000**, *16* (4), 1806–1815.
- (35) Reviakine, I.; Brisson, A. Streptavidin 2D crystals on supported phospholipid bilayers: Toward constructing anchored phospholipid bilayers. *Langmuir* **2001**, *17* (26), 8293–8299.
- (36) Horton, M. R.; Reich, C.; Gast, A. P.; Radler, J. O.; Nickel, B. Structure and dynamics of crystalline protein layers bound to supported lipid bilayers. *Langmuir* **2007**, *23* (11), 6263–6269.
- (37) Parthasarathy, R.; Groves, J. T. Protein patterns at lipid bilayer junctions. *Proc. Natl. Acad. Sci. U. S. A.* **2004**, *101* (35), 12798–12803.
- (38) Glasmästar, K.; Larsson, C.; Hook, F.; Kasemo, B. Protein adsorption on supported phospholipid bilayers. *J. Colloid Interface Sci.* **2002**, *246* (1), 40–47.
- (39) Rossetti, F. F.; Textor, M.; Reviakine, I. Asymmetric distribution of phosphatidyl serine in supported phospholipid bilayers on titanium dioxide. *Langmuir* **2006**, *22* (8), 3467–3473.
- (40) Andersson, A. S.; Glasmästar, K.; Sutherland, D.; Lidberg, U.; Kasemo, B. Cell adhesion on supported lipid bilayers. *J. Biomed. Mater. Res., Part A* **2003**, *64A* (4), 622–629.
- (41) Braune, S.; Walter, M.; Schulze, F.; Lendlein, A.; Jung, F. Changes in platelet morphology and function during 24 h of storage. *Clin. Hemorheol. Microcirc.* **2014**, *58* (1), 159–70.
- (42) Dijkstra-Tiekstra, M. J.; van der Meer, P. F.; Cardigan, R.; Devine, D.; Prowse, C.; Sandgren, P.; de Wildt-Eggen, J. Platelet concentrates from fresh or overnight-stored blood, an international study. *Transfusion* **2011**, *51*, 38S–44S.
- (43) van der Meer, P. F.; Cancelas, J. A.; Vassallo, R. R.; Rugg, N.; Einarson, M.; Hess, J. R. Evaluation of the overnight hold of whole blood at room temperature, before component processing: platelets (PLTs) from PLT-rich plasma. *Transfusion* **2011**, *51*, 45S–49S.
- (44) Persson, F.; Fritzsche, J.; Mir, K. U.; Modesti, M.; Westerlund, F.; Tegenfeldt, J. O. Lipid-Based Passivation in Nanofluidics. *Nano Lett.* **2012**, *12* (5), 2260–2265.
- (45) Groves, J. T.; Dustin, M. L. Supported planar bilayers in studies on immune cell adhesion and communication. *J. Immunol. Methods* **2003**, *278* (1–2), 19–32.
- (46) Mossman, K.; Groves, J. Micropatterned supported membranes as tools for quantitative studies of the immunological synapse. *Chem. Soc. Rev.* **2007**, *36* (1), 46–54.
- (47) Torres, A. J.; Contento, R. L.; Gordo, S.; Wucherpfennig, K. W.; Love, J. C. Functional single-cell analysis of T-cell activation by supported lipid bilayer-tethered ligands on arrays of nanowells. *Lab Chip* **2013**, *13* (1), 90–9.
- (48) Macdonald, R. C.; Macdonald, R. I.; Menco, B. P. M.; Takeshita, K.; Subbarao, N. K.; Hu, L. R. Small-volume extrusion apparatus for preparation of large, unilamellar vesicles. *Biochim. Biophys. Acta, Biomembr.* **1991**, *1061* (2), 297–303.
- (49) Hain, N.; Gallego, M.; Reviakine, I. Unraveling Supported Lipid Bilayer Formation Kinetics: Osmotic Effects. *Langmuir* **2013**, *29* (7), 2282–2288.
- (50) Zhu, L.; Gregurec, D.; Reviakine, I. Nanoscale departures: excess lipid leaving the surface during supported lipid bilayer formation. *Langmuir* **2013**, *29* (49), 15283–92.
- (51) Gupta, S. *Selective Activation of Platelets by Surfaces and Soluble Agonists*. Ph.D. thesis, University of the Basque Country, 2014.
- (52) Michelson, A. D.; Barnard, M. R.; Krueger, L. A.; Frelinger, A. L., 3rd; Furman, M. I. Evaluation of platelet function by flow cytometry. *Methods* **2000**, *21* (3), 259–70.
- (53) Michelson, A. D.; Barnard, M. R.; Krueger, L. A.; Valeri, C. R.; Furman, M. I. Circulating monocyte-platelet aggregates are a more sensitive marker of in vivo platelet activation than platelet surface P-selectin: studies in baboons, human coronary intervention, and human acute myocardial infarction. *Circulation* **2001**, *104* (13), 1533–7.
- (54) Rossetti, F. F.; Reviakine, I.; Csucs, G.; Assi, F.; Voros, J.; Textor, M. Interaction of poly(L-lysine)-g-poly(ethylene glycol) with supported phospholipid bilayers. *Biophys. J.* **2004**, *87* (3), 1711–1721.
- (55) Balasubramanian, K.; Schroit, A. J. Aminophospholipid asymmetry: A matter of life and death. *Annu. Rev. Physiol.* **2003**, *65*, 701–734.
- (56) Seigneuret, M.; Devaux, P. F. ATP-dependent asymmetric distribution of spin-labeled phospholipids in the erythrocyte membrane: relation to shape changes. *Proc. Natl. Acad. Sci. U. S. A.* **1984**, *81* (12), 3751–5.
- (57) Daleke, D. L. Regulation of transbilayer plasma membrane phospholipid asymmetry. *J. Lipid Res.* **2003**, *44* (2), 233–242.
- (58) Morrot, G.; Herve, P.; Zachowski, A.; Fellmann, P.; Devaux, P. F. Aminophospholipid translocase of human erythrocytes: phospholipid substrate specificity and effect of cholesterol. *Biochemistry* **1989**, *28* (8), 3456–3462.
- (59) Cremer, P. S.; Groves, J. T.; Kung, L. A.; Boxer, S. G. Writing and erasing barriers to lateral mobility into fluid phospholipid bilayers. *Langmuir* **1999**, *15* (11), 3893–3896.
- (60) Hovis, J. S.; Boxer, S. G. Patterning barriers to lateral diffusion in supported lipid bilayer membranes by blotting and stamping. *Langmuir* **2000**, *16* (3), 894–897.
- (61) Kung, L. A.; Kam, L.; Hovis, J. S.; Boxer, S. G. Patterning hybrid surfaces of proteins and supported lipid bilayers. *Langmuir* **2000**, *16* (17), 6773–6776.
- (62) Hovis, J. S.; Boxer, S. G. Patterning and composition arrays of supported lipid bilayers by microcontact printing. *Langmuir* **2001**, *17* (11), 3400–3405.
- (63) Rossetti, F. F.; Bally, M.; Michel, R.; Textor, M.; Reviakine, I. Interactions between Titanium Dioxide and Phosphatidyl Serine-containing Liposomes: Formation and Patterning of Supported Phospholipid Bilayers on the Surface of a Medically Relevant Material. *Langmuir* **2005**, *21*, 6443–6450.
- (64) Jonsson, P.; Beech, J. P.; Tegenfeldt, J. O.; Hook, F. Mechanical Behavior of a Supported Lipid Bilayer under External Shear Forces. *Langmuir* **2009**, *25* (11), 6279–6286.
- (65) Reimhult, E.; Baumann, M. K.; Kaufmann, S.; Kumar, K.; Spycher, P. R. Advances in Nanopatterned and Nanostructured Supported Lipid Membranes and Their Applications. *Biotechnology and Genetic Engineering Reviews*; Nottingham University Press: Loughborough, 2010; Vol. 27, pp 185–216.
- (66) Hansson, K. M.; Tosatti, S.; Isaksson, J.; Wettero, J.; Textor, M.; Lindahl, T. L.; Tengvall, P. Whole blood coagulation on protein adsorption-resistant PEG and peptide functionalised PEG-coated titanium surfaces. *Biomaterials* **2005**, *26* (8), 861–872.
- (67) Riedel, T.; Riedelova-Reicheltova, Z.; Majek, P.; Rodriguez-Emmenegger, C.; Houska, M.; Dyr, J. E.; Brynda, E. Complete identification of proteins responsible for human blood plasma fouling on poly(ethylene glycol)-based surfaces. *Langmuir* **2013**, *29* (10), 3388–97.
- (68) Kiessling, V.; Wan, C.; Tamm, L. K. Domain coupling in asymmetric lipid bilayers. *Biochim. Biophys. Acta, Biomembr.* **2009**, *1788* (1), 64–71.
- (69) Verkleij, A. J.; Zwaal, R. F. A.; Roelofse, B.; Comfurui, P.; Kastelij, D.; Vandeene, L. Asymmetric Distribution of Phospholipids in Human Red-Cell Membrane - Combined Study Using Phospholipases and Freeze-Etch Electron-Microscopy. *Biochim. Biophys. Acta, Biomembr.* **1973**, *323* (2), 178–193.